Introducing screening in one-body density matrix functionals: Impact on charged excitations of model systems via the extended Koopmans' theorem

S. Di Sabatino[1,2] J. Koskelo,[2] J. A. Berger,[1] and P. Romaniello[2]

[1]*Laboratoire de Chimie et Physique Quantiques, Université de Toulouse, CNRS, UPS and ETSF, F-31062 Toulouse, France*
[2]*Laboratoire de Physique Théorique, Université de Toulouse, CNRS, UPS and ETSF, F-31062 Toulouse, France*

In this work we get insight into the impact of reduced density matrix functionals on the quality of removal/addition energies obtained using the extended Koopmans' theorem (EKT). Within the reduced density matrix functional theory (RDMFT) the EKT approach reduces to a matrix diagonalization, whose ingredients are the one- and two-body reduced density matrices. A striking feature of the EKT within RDMFT is that it opens a band gap, although it is too large, in strongly correlated materials, which are a challenge for state-of-the-art methods such as *GW*. Using the one-dimensional Hubbard model and the homogeneous electron gas as test cases, we find that (i) with exact or very accurate density matrices the EKT systematically overestimates the band gap in the Hubbard model and the bandwidth in the homogeneous electron gas and (ii) with approximate density matrices, instead, the EKT can benefit from error cancellation. In particular we test a new approximation which combines random-phase approximation screening with the power functional approximation to the two-body reduced density matrix introduced by Sharma *et al.* [Phys. Rev. B **78**, 201103 (2008)]. An important feature of this approximation is that it reduces the EKT band gap in the studied models; it is hence a promising approximation for correcting the EKT band-gap overestimation in strongly correlated materials.

I. INTRODUCTION

The extended Koopmans' theorem (EKT) [1,2] offers an interesting tool for the calculation of removal/addition energies from any level of theory [3–6]. In particular within reduced density matrix functional theory (RDMFT) [7–9], the EKT approach is based on a matrix diagonalization, whose ingredients are the one- and two-body reduced density matrices (1-RDM and 2-RDM, respectively). This formulation is particularly appealing because it relies not on the knowledge of the ground-state many-body wave function of the *N*-electron system but on simpler quantities, namely, the natural orbitals and occupation numbers, i.e., the eigenvectors and eigenvalues of the 1-RDM. Within RDMFT, indeed, the one-body reduced density matrix, thanks to a one-to-one map with the ground-state many-body wave function, can give access to all ground-state observables of the system, provided that their functional expression in terms of the 1-RDM is known. In particular the total energy is a functional of the 1-RDM, and its minimization under a set of physical constraints (ensemble *N*-representable constraints) gives the exact 1-RDM. In practice the electron-electron interaction energy, which can be expressed in terms of the 2-RDM, is an unknown functional (more precisely, its correlation part) of the 1-RDM, and approximations are needed. The EKT offers a path towards the description of photoemission in strongly correlated materials, which is a challenge for *ab initio* theories. We have indeed shown that EKT energies within the so-called diagonal approximation (DEKT) [10] are equivalent to the energies obtained within the many-body effective energy theory

(MEET) [11] at its lowest-order approximation in terms of the 1-RDM and 2-RDM. At this level of approximation and within RDMFT the MEET gives a qualitatively good description of the photoemission spectra of several paramagnetic transition-metal oxides, which are insulators, unlike mean-field theories and the more advanced *GW* method, which describe them as metals [11–13]. The band gap, however, is largely overestimated. There are, indeed, two sources of error in the EKT. One source is the structure of the EKT equations: even with exact 1- and 2-RDM an overestimation of the band gap (small for weakly correlated systems, larger for strongly correlated systems) is expected. We recently addressed this issue with the example of bulk Si [10]. The EKT with quantum Monte Carlo (QMC) density matrices overestimates the band gap of ≈1 eV. To overcome this error one should go beyond the EKT equations and include higher-order density matrices, which makes the approach more expensive. Another option is to work with an effective 2-RDM which partially includes the effect of higher-order terms. This work is in progress. The second source of error is the approximate one- and two-body density matrices used in the EKT equations. The band-gap overestimation can be amplified by commonly used approximations to the two-body density matrix employed in RDMFT. In particular we used the power functional (PF) proposed by Sharma *et al.* [14], which is the only one that, to the best of our knowledge, has been used in solids, but similar trends are expected using approximations of the same type, i.e., the so-called $\mathcal{JK}$ functionals, which involve only Coulomb-like ($\mathcal{J}$) and exchange-like ($\mathcal{K}$) integrals involving the natural orbitals [15]. Therefore in this work we propose

a variation of the PF in which random-phase approximation (RPA) screening is taken into account, referred to as screened PF (W-PF) throughout this paper. This is motivated by the fact that in many-electron systems screening becomes important and, for example, in the context of many-body perturbation theory (MBPT) based on Green's functions the improvement of the GW approximation over Hartree-Fock is precisely due to the screening of the Coulomb interaction. We also consider the corrected Buijse-Baerends (BBC1) functional proposed by Gritsenko *et al.* [16], which, as we shall see, shows important physical features in the correlation energy and the natural orbital occupation numbers, which can have an impact on the quality of the EKT removal/addition energies. We test the quality of these approximations using the one-dimensional Hubbard model and the homogeneous electron gas (HEG) as benchmark systems.

This paper is organized as follows. In Sec. II we give the basic equations of the EKT as well as RDMFT, and we derive the W-PF. In Sec. III we describe the two models used. Computational details are discussed in Sec. IV. In Sec. V we report and discuss our results. In Sec. VI we draw our conclusions and perspectives.

II. THEORETICAL FRAMEWORK

A. The extended Koopman's theorem

Within the EKT we consider the following wave functions for the νth one-particle removal excitations [3]:

$$\left|\Psi_\nu^{N-1}\right\rangle = \hat{O}_\nu\left|\Psi_0^N\right\rangle, \tag{1}$$

where $\left|\Psi_0^N\right\rangle$ is the N-particle ground-state wave function, $\hat{O}_\nu$ is the electron annihilation operator $\hat{O}_\nu = \sum_i C_{\nu i}^R \hat{c}_i$, and $\{C_{\nu i}^R\}$ are a set of coefficients to be determined. Here the indices $i, j, \ldots$ refer to a general basis of spin orbitals; that is, $i = I\sigma$ comprises the orbital index I and the spin σ. The corresponding removal energy is given by

$$\epsilon_\nu^R = -\frac{\left\langle\Psi_0^N\left|\hat{O}_\nu^\dagger[\hat{H}, \hat{O}_\nu]\right|\Psi_0^N\right\rangle}{\left\langle\Psi_0^N\left|\hat{O}_\nu^\dagger\hat{O}_\nu\right|\Psi_0^N\right\rangle}. \tag{2}$$

The stationary condition (with respect to the coefficients $C_{\nu i}^R$) for ϵ_i^R leads to the following generalized eigenvalue equation:

$$\left(\mathbf{F}^R - \epsilon_\nu^R\mathbf{S}^R\right)\mathbf{C}_\nu^R = 0, \tag{3}$$

with $F_{ij}^R = -\langle\Psi_0^N|\hat{c}_j^\dagger[\hat{H}, \hat{c}_i]|\Psi_0^N\rangle$ and $\mathbf{S}^R$ being the one-body reduced density matrix $S_{ij}^R = \gamma_{ij} = \langle\Psi_0^N|\hat{c}_j^\dagger\hat{c}_i|\Psi_0^N\rangle$. If one defines the matrix $\mathbf{\Lambda}^R = [\mathbf{S}^R]^{-1}\mathbf{F}^R$ in the basis of natural orbitals, with $S_{ij}^R = n_i\delta_{ij}$, and works out the commutator in F_{ij}^R using the many-body Hamiltonian $\hat{H} = \sum_{ij} h_{ij}\hat{c}_i^\dagger\hat{c}_j + \frac{1}{2}\sum_{ijkl} V_{ijkl}\hat{c}_i^\dagger\hat{c}_j^\dagger\hat{c}_l\hat{c}_k$, one arrives at

$$\Lambda_{ij}^R = \frac{1}{n_i}\left[n_i h_{ji} + \sum_{klm} V_{jmkl}\Gamma_{klmi}^{(2)}\right], \tag{4}$$

where $\Gamma_{klji}^{(2)} = \langle\Psi_0^N|\hat{c}_i^\dagger\hat{c}_j^\dagger\hat{c}_l\hat{c}_k|\Psi_0^N\rangle$ are the 2-RDM matrix elements; $h_{ij} = \int d\mathbf{x}\phi_i^*(\mathbf{x})h(\mathbf{x})\phi_j(\mathbf{x})$ are the matrix elements of the one-particle noninteracting Hamiltonian $h(\mathbf{x}) = -\nabla^2/2 +$

$v_{\text{ext}}(\mathbf{x})$, with $v_{\text{ext}}(\mathbf{x})$ being a static external potential; and $V_{ijkl} = \int d\mathbf{x}d\mathbf{x}'\phi_i^*(\mathbf{x})\phi_j^*(\mathbf{x}')v(\mathbf{x}, \mathbf{x}')\phi_k(\mathbf{x})\phi_l(\mathbf{x}')$ are the matrix elements of the Coulomb interaction $v(\mathbf{x}, \mathbf{x}')$. Diagonalization of $\mathbf{\Lambda}^R$ yields the removal energies ϵ_ν^R as eigenvalues [1,5]. The diagonal elements of $\mathbf{\Lambda}^R$ are referred to in the literature as the energies of the EKT within the diagonal approximation (DEKT) [3].

Similar equations hold for the addition energies. We can, indeed, start from the wave function $|\Psi_\nu^{N+1}\rangle = \hat{O}_\nu^\dagger|\Psi_0^N\rangle$, with $\hat{O}_\nu^\dagger = \sum_i C_{\nu i}^A\hat{c}_i^\dagger$, and write the addition energy ϵ_ν^A as

$$\epsilon_\nu^A = \frac{\left\langle\Psi_0^N\left|[\hat{H}, \hat{O}_\nu]\hat{O}_\nu^\dagger\right|\Psi_0^N\right\rangle}{\left\langle\Psi_0^N\left|\hat{O}_\nu\hat{O}_\nu^\dagger\right|\Psi_0^N\right\rangle}, \tag{5}$$

and in a way similar to that for ϵ_ν^R we arrive at the generalized eigenvalue equation

$$\left(\mathbf{F}^A - \epsilon_\nu^A\mathbf{S}^A\right)\mathbf{C}_\nu^A = 0, \tag{6}$$

where $F_{ij}^A = \langle\Psi_0^N|\hat{c}_i[\hat{H}, \hat{c}_j^\dagger]|\Psi_0^N\rangle$ and $\mathbf{S}^A$ is related to the one-body density matrix as $S_{ij}^A = 1 - \gamma_{ij}$. Like for the removal energy problem, using the basis of natural orbitals, we can work out the commutator in F_{ij}^A and reformulate the problem in terms of the matrix $\mathbf{\Lambda}^A = [\mathbf{S}^A]^{-1}\mathbf{F}^A$ [17], which reads

$$\Lambda_{ij}^A = \frac{1}{(1-n_i)}\Bigg[(1-n_i)h_{ji} + \sum_k (V_{jkik} - V_{jkki})n_k$$
$$\times -\sum_{klm} V_{jmkl}\Gamma_{klmi}^{(2)}\Bigg]. \tag{7}$$

Diagonalization of $\mathbf{\Lambda}^A$ yields the addition energies ϵ_ν^A as eigenvalues. The EKT approach offers a way to build approximations for the spectral function, which is linked to the photoemission spectrum [4,10,18]. In the basis of natural orbitals and within the DEKT the approximate spectral function assumes a particular simple form given by

$$A(\omega) = \sum_i \left[n_i\delta\left(\omega - \epsilon_i^R\right) + (1-n_i)\delta\left(\omega - \epsilon_i^A\right)\right]. \tag{8}$$

B. RDMFT

In RDMFT the ground-state total energy is a unique functional of the 1-RDM,

$$E[\gamma] = \int d\mathbf{x}d\mathbf{x}'\delta(\mathbf{x} - \mathbf{x}')h(\mathbf{x})\gamma(\mathbf{x}, \mathbf{x}')$$
$$+ \frac{1}{2}\int d\mathbf{x}d\mathbf{x}'v(\mathbf{x}, \mathbf{x}')\Gamma^{(2)}[\gamma](\mathbf{x}, \mathbf{x}'; \mathbf{x}, \mathbf{x}'), \tag{9}$$

where the 2-RDM can be factorized as

$$\Gamma^{(2)}[\gamma](\mathbf{x}, \mathbf{x}'; \mathbf{x}, \mathbf{x}') = \gamma(\mathbf{x}, \mathbf{x})\gamma(\mathbf{x}', \mathbf{x}') - \gamma(\mathbf{x}, \mathbf{x}')\gamma(\mathbf{x}', \mathbf{x})$$
$$+ \Gamma_c^{(2)}[\gamma](\mathbf{x}, \mathbf{x}'; \mathbf{x}, \mathbf{x}'). \tag{10}$$

The first and second terms on the right-hand side of Eq. (10) give rise to the Hartree and exchange contributions to the total energy, whereas the last term yields the correlation energy, which is the only unknown part and which needs to be approximated. Most of the commonly used approximations are implicit functionals of the 1-RDM and explicit functionals of the natural orbitals ϕ_i and occupation numbers n_i, which are

the eigenvectors and eigenvalues, respectively, of the 1-RDM [i.e., $\gamma(\mathbf{x}, \mathbf{x}') = \sum_i n_i \phi_i(\mathbf{x})\phi_i^*(\mathbf{x}')$]. In particular here we focus on the $\mathcal{JK}$-only functionals, which, in their simplest form, read

$$\Gamma^{(2)}[\gamma](\mathbf{x}, \mathbf{x}'; \mathbf{x}, \mathbf{x}')$$
$$\approx \sum_{ij} n_i n_j \phi_i^*(\mathbf{x})\phi_j^*(\mathbf{x}')\phi_i(\mathbf{x})\phi_j(\mathbf{x}')$$
$$- \sum_{ij} f(n_i, n_j)\phi_i^*(\mathbf{x})\phi_j^*(\mathbf{x}')\phi_j(\mathbf{x})\phi_i(\mathbf{x}'); \quad (11)$$

that is, they have the form of the Hartree-Fock exchange modified by the function $f(n_i, n_j)$ of the occupation numbers.

In this work we will focus on the PF proposed by Sharma *et al.* [14,18], which is the only one that, to the best of our knowledge, has been used in solids, for which $f^{\mathrm{PF}}(n_i, n_j) = n_i^\alpha n_j^\alpha$, with $0.5 \leqslant \alpha \leqslant 1$. Note that with $\alpha = 1$ one gets the Hartree-Fock approximation to $\Gamma^{(2)}$, whereas with $\alpha = 0.5$ one gets the Müller functional [19]. We will also employ the BBC1 functional [16] for which one has to distinguish between strongly and weakly occupied orbitals. This distinction appears naturally when a subset of the orbitals corresponds to occupation numbers close to 1 and the rest correspond to occupation numbers close to 0 (weakly correlated systems). However, in more general situations this distinction might be an issue. Here we will use the simplest version of the BBC functional, BBC1, for which

$$f^{\mathrm{BBC1}}(n_i, n_j)$$
$$= \begin{cases} -\sqrt{n_i n_j} & \text{if } I \neq J \text{ and } i, j \text{ weakly occupied,} \\ \sqrt{n_i n_j} & \text{otherwise.} \end{cases} \quad (12)$$

Extension of more advanced functionals used for finite systems to solids, such as some of the Piris Natural Orbital functional (PNOF) series [20–22], is not straightforward.

The total energy can then be expressed as a functional of ϕ_i and n_i, $E[\{n_i\}, \{\phi_i\}]$; functional minimization with respect to the natural orbitals, under orthonormality constraints, and occupation numbers, under the ensemble N-representability constraints ($\sum_i n_i = N$, with N being the total number of electrons, and $0 \leqslant n_i \leqslant 1$), leads to the ground-state total energy.

1. Screened power functional

In the expressions for the RDMFT total energy and for the EKT energies we have terms like

$$\sum_{klm} V_{jmkl} \Gamma^{(2)}_{klmi}. \quad (13)$$

In the following we exploit the link between $\Gamma^{(2)}$ and the two-body Green's function $G^{(2)}$ [23],

$$\Gamma^{(2)}(\mathbf{x}_1, \mathbf{x}_2; \mathbf{x}_1', \mathbf{x}_2) = -G^{(2)}(\mathbf{x}_1 t_1, \mathbf{x}_2 t_1^+; \mathbf{x}_1' t_1^{+++}, \mathbf{x}_2 t_1^{++}),$$

with $t_1^+ = t_1 + \delta$ ($\delta = 0^+$), to get an approximation to $\Gamma^{(2)}$ from approximations to the self-energy Σ of MBPT. We first start from the definition of the self-energy in terms of $G^{(2)}$:

$$\int d2\, \Sigma(12)G(24) = -i \int d3\, v(13)G^{(2)}(13^+; 43^{++}), \quad (14)$$

where $1 \equiv (\mathbf{x}_1, t_1)$ is a space-spin plus time composite variable. By expressing G and $G^{(2)}$ in a basis set $\{\phi_i(\mathbf{x})\}$ and by multiplying and integrating both sides of the equation with $\int d\mathbf{x}_1 d\mathbf{x}_4 \phi_m^*(\mathbf{x}_1)\phi_l(\mathbf{x}_4)$, we arrive at

$$\sum_i \int dt_2\, \Sigma_{mi}(t_1 t_2)G_{il}(t_2 t_4) = -i \sum_{ijk} V_{mkij} G^{(2)}_{ijkl}(t_1 t_1^+; t_4 t_1^{++}), \quad (15)$$

with $G_{ij}(t_1 t_2) = -i\langle \Psi_0 | \mathcal{T}[\hat{c}_i(t_1)\hat{c}_j^\dagger(t_2)] | \Psi_0 \rangle$ and $G^{(2)}_{ijkl}(t_1 t_2; t_3 t_4) = -\langle \Psi_0 | \mathcal{T}[\hat{c}_i(t_1)\hat{c}_j(t_2)\hat{c}_k^\dagger(t_4)\hat{c}_l^\dagger(t_3)] | \Psi_0 \rangle$. We now consider $t_4 = t_1^{+++}$ to get $\Gamma^{(2)}$ on the right-hand side. Expressing the left-hand side in frequency space, we arrive at

$$\sum_i \int \frac{d\omega}{2\pi} \Sigma_{mi}(\omega)G_{il}(\omega)e^{i\omega\eta} = i \sum_{ijk} V_{mkij}\Gamma^{(2)}_{ijkl}. \quad (16)$$

Approximations to the self-energy will give approximations to the term $V\Gamma^{(2)}$. In particular the frequency dependence of the self-energy is essential to have fractional occupation numbers [24], which in turn are related to the band-gap opening in strongly correlated systems [11]. However, modeling the correct frequency dependence is not easy. As a paradigmatic example we can consider the Hubbard dimer, in which the well-known GW approximation to the self-energy fails to open a gap in the strongly correlated limit [11]. We therefore consider a static self-energy, such as GW with a statically screened W, which leads to

$$\sum_{ijk} \gamma_{kj} W_{mjki} \gamma_{il} = -\sum_{ijk} V_{mkij}\Gamma^{(2)}_{\mathrm{xc},ijkl}, \quad (17)$$

where we used the fact that $-i \int d\omega/(2\pi)G_{il}(\omega)e^{i\omega\eta} = \gamma_{il}$ and where we considered only the exchange-correlation contributions to Σ and $\Gamma^{(2)}$ since the Hartree contribution to $\Gamma^{(2)}$ as a functional of the 1-RDM is known. If we work in the basis of natural orbitals, we get

$$\sum_j W_{mjjl} n_j n_l = -\sum_{ijk} V_{mkij}\Gamma^{(2)}_{\mathrm{xc},ijkl}. \quad (18)$$

For $W = v$ this is the exchange approximation. Using a static W corresponds to the screened exchange (SEX) approximation, which, like Hartree-Fock (HF), leads to occupation numbers equal to 0 or 1. In order to get fractional occupation numbers we combine this approximation with the power functional to get the screened power functional

$$\sum_j W_{mjjl} n_j^\alpha n_l^\alpha = -\sum_{ijk} V_{mkij}\Gamma^{(2)}_{\mathrm{xc},ijkl}, \quad (19)$$

where W has to be considered fixed (which, hence, does not enter into the variational process). The rationale behind this approximation is that the PF will describe strong correlation (or nondynamic correlation, related to the existence of quasidegenerate states), whereas a static W will describe weak correlation (or dynamic correlation, related to electron screening). Of course, double-counting problems are possible, as we shall see when discussing the results. In the following we will refer to this approximations as W-PF. This derivation can also be extended to the Coulomb hole + screened exchange (COHSEX) approximation [25–28], which is more commonly used in many-body perturbation theory. This is shown in

Appendix A. The final result is similar to Eq. (19) with an extra term taking into account the Coulomb hole (COH).

III. MODELS

To test the quality of the W-PF we use two well-known models in condensed-matter physics, namely, the one-dimensional Hubbard model and the HEG.

A. One-dimensional Hubbard model

In this work we will consider a Hubbard chain with number of sites L and periodic boundary conditions. The Hamiltonian of the Hubbard model, in second quantization, reads

$$\hat{H} = -t \sum_{\langle R,R' \rangle} \sum_\sigma \hat{c}^\dagger_{R\sigma} \hat{c}_{R'\sigma} + \frac{U}{2} \sum_R \sum_{\sigma\sigma'} \hat{c}^\dagger_{R\sigma} \hat{c}^\dagger_{R\sigma'} \hat{c}_{R\sigma'} \hat{c}_{R\sigma}. \quad (20)$$

Here $\hat{c}^\dagger_{R\sigma}$ and $\hat{c}_{R\sigma}$ are the creation and annihilation operators for an electron at site R with spin σ, U is the on-site (spin-independent) interaction, $-t$ is the hopping kinetic energy. The summation $\sum_{\langle R,R' \rangle}$ is restricted to the nearest-neighbor sites. Due to the translational invariance of the system the natural orbitals have the form $\phi_{I\sigma} = \frac{1}{\sqrt{L}} \sum_R e^{iIR} \varphi_{R\sigma}$, where $\varphi_{R\sigma}$ are the site spin orbitals, and the total energy is a function of the occupation numbers alone, which reads [29]

$$E[\{n_{I\sigma}\}] = \sum_I \sum_\sigma \epsilon^0_I n_{I\sigma} + \frac{U}{4} \sum_{IJ} \sum_{\sigma\sigma'} n_{I\sigma} n_{J\sigma'}$$
$$- \frac{U}{4} \sum_{IJ} \sum_\sigma n^\alpha_{I\sigma} n^\alpha_{J\sigma}, \quad (21)$$

where $\epsilon^0_I = -2t \cos[2\pi(I-1)/L]$ is the noninteracting energy associated with the Ith natural orbital [30] and we used the PF to approximate Γ_{xc}, with $0.5 \leqslant \alpha \leqslant 1$ [14]. In this work we considered only the spin-symmetric case at one-half filling.

B. HEG

The HEG Hamiltonian in its spin-explicit form is given by the following expression:

$$\hat{H} = \sum_\sigma \sum_{\mathbf{k}} \frac{\mathbf{k}^2}{2} \hat{c}^\dagger_{\mathbf{k},\sigma} \hat{c}_{\mathbf{k},\sigma} + \frac{1}{2\Omega} \sum_{\sigma\sigma'} \sum_{\mathbf{k} \neq 0, \mathbf{k}_1, \mathbf{k}_2}$$
$$\times \frac{4\pi}{\mathbf{k}^2} \hat{c}^\dagger_{\mathbf{k}_1+\mathbf{k},\sigma} \hat{c}^\dagger_{\mathbf{k}_2-\mathbf{k},\sigma'} \hat{c}_{\mathbf{k}_2,\sigma'} \hat{c}_{\mathbf{k}_1,\sigma} + E_b, \quad (22)$$

where $\mathbf{k}$ is a plane wave vector and Ω is the volume of the unit cell. Note that to guarantee the charge neutrality of the system a positive background charge has to be included. This results in the constant term E_b in the Hamiltonian, which contains the electron-background interactions.

Due to the translational invariance of the HEG, the natural orbitals can be chosen to be plane waves. The minimization procedure reduces then to the search for the optimal momentum distribution $n(\mathbf{k})$, i.e., the occupation number corresponding to the plane-wave natural orbital with wave vector $\mathbf{k}$. We also note that, due to the rotational invariance, $n(\mathbf{k}) = n(k)$, i.e., the momentum distribution depends only on the magnitude of $\mathbf{k}$.

The total energy functional per unit volume can be expressed in terms of the momentum distribution as

$$\frac{E}{\Omega} = \int \frac{d\mathbf{k}}{(2\pi)^3} \mathbf{k}^2 n(\mathbf{k}) - \int \frac{d\mathbf{k} d\mathbf{k}'}{(2\pi)^6} v(\mathbf{k}-\mathbf{k}') f(n(\mathbf{k}), n(\mathbf{k}')), \quad (23)$$

where the first and second terms on the right-hand side are the kinetic energy and the exchange-correlation energy per unit of volume, respectively, and $v(\mathbf{k}) = 4\pi/|\mathbf{k}|^2$ is the Coulomb potential. Note that the Hartree energy is not included in Eq. (23) since it is compensated by E_b. RDMFT functionals have already been applied to the homogeneous electron gas [31–34]. In particular Lathiotakis *et al.* [31] studied the performance of the BBC functionals for the correlation energies and the momentum distribution. Within the PF approximation to the 2-RDM we have $f^{\text{PF}}(n(\mathbf{k}), n(\mathbf{k}')) = [n(\mathbf{k})n(\mathbf{k}')]^\alpha$ with $0.5 \leqslant \alpha \leqslant 1$ [14], while for the BBC1 functional we have $f^{\text{BBC1}}(n(\mathbf{k}), n(\mathbf{k}')) = \sqrt{n(\mathbf{k})n(\mathbf{k}')}[1 - 2\theta(|\mathbf{k}| - k_F)\theta(|\mathbf{k}'| - k_F)]$, where θ is the Heaviside step function. Within the screened power functional approximation, instead, $f^{W\text{-PF}}(n(\mathbf{k}), n(\mathbf{k}')) = \bar{W}(\mathbf{k} - \mathbf{k}')/v(\mathbf{k} - \mathbf{k}')[n(\mathbf{k})n(\mathbf{k}')]^\alpha$; that is, the Coulomb potential $v(\mathbf{k})$ in the PF is replaced by the screened interaction $\bar{W}(\mathbf{k})$. In the following we will assume that $\bar{W}$ is the static limit of the dynamically screened interaction W, given by

$$\bar{W}(\mathbf{k}) = \frac{v(\mathbf{k})}{1 - v(\mathbf{k})P^0(0, \mathbf{k})}, \quad (24)$$

with the static RPA polarizability given by the Lindhard formula [35]

$$P^0(0, \mathbf{k}) = \frac{2k_F}{4\pi^2} \left\{ -1 + \frac{k_F}{2k}\left(1 - \frac{k^2}{4k_F^2}\right) \ln\left[\frac{1 - k/(2k_F)}{1 + k/(2k_F)}\right]^2 \right\}, \quad (25)$$

where k_F is the Fermi momentum, given by $k_F = (9\pi/4)^{1/3}/r_s$, and r_s is the Wigner radius.

For the HEG, the matrices given in Eqs. (4) and (7) are diagonal in the basis of natural orbitals, and their diagonal elements are the EKT removal and addition energies, respectively, given by

$$\epsilon^R(\mathbf{k}) = \frac{k^2}{2} - \frac{1}{n(\mathbf{k})} \int \frac{d\mathbf{k}'}{(2\pi)^3} v(\mathbf{k} - \mathbf{k}') f(n(\mathbf{k}), n(\mathbf{k}')) \quad (26)$$

and

$$\epsilon^A(\mathbf{k}) = \frac{k^2}{2} - \frac{1}{1 - n(\mathbf{k})} \int \frac{d\mathbf{k}'}{(2\pi)^3} v(\mathbf{k} - \mathbf{k}') n(\mathbf{k}')$$
$$+ \frac{1}{1 - n(\mathbf{k})} \int \frac{d\mathbf{k}'}{(2\pi)^3} v(\mathbf{k} - \mathbf{k}') f(n(\mathbf{k}), n(\mathbf{k}')), \quad (27)$$

where we used the approximation in Eq. (11) for the 2-RDM.

IV. COMPUTATIONAL DETAILS

For the Hubbard model with a finite number of sites we use the Lanczos method [36] for the calculation of the exact one-body Green's function, from which we get all the quantities of interest for this work. This poses a limit to the number of sites we can treat, which in our case is $L = 12$. For the infinite chain

$(L \rightarrow \infty)$ we use the Bethe ansatz [37]. For the total energy minimization within the approximate power functional we use the direct minimization for finite sites using the *Mathematica* package [38]. In the case of the infinite chain, instead, we use the same strategy used for the HEG, which we describe in the following.

For the HEG, the functional to be minimized can be written as [31]

$$\frac{\mathcal{F}}{\Omega} = \int \frac{d\mathbf{k}}{(2\pi)^3} (\mathbf{k}^2 - 2\mu) n(\mathbf{k})$$
$$- \int \frac{d\mathbf{k} d\mathbf{k}'}{(2\pi)^6} v(\mathbf{k} - \mathbf{k}') f(n(\mathbf{k}), n(\mathbf{k}')) + \mu, \quad (28)$$

where μ is the Lagrange multiplier which enforces the condition $\sum_i n_i = N$. From the stationarity condition

$$\frac{\delta(\mathcal{F}/\Omega)}{\delta n(\mathbf{k})} = \frac{1}{(2\pi)^3} (\mathbf{k}^2 - 2\mu)$$
$$- 2 \int \frac{d\mathbf{k}'}{(2\pi)^6} v(\mathbf{k} - \mathbf{k}') \partial_x f(x, n(\mathbf{k}')) \big|_{x=n(\mathbf{k})}$$
$$= 0, \quad (29)$$

and using the PF approximation (i.e., $f(n(\mathbf{k}), n(\mathbf{k}')) = [n(\mathbf{k}) n(\mathbf{k}')]^{\alpha}$), we can obtain the following integral equation [39]:

$$n(\mathbf{k}) = \left\{ \frac{\int d\mathbf{k}'/(2\pi)^3 v(\mathbf{k} - \mathbf{k}')[n(\mathbf{k}')]^{\alpha}}{\mathbf{k}^2/2 - \mu} \right\}^{\frac{1}{1-\alpha}}. \quad (30)$$

Similar equations can be obtained using the BBC1 functional and the W-PF. The minimization of the energy functional is thus transformed into a fixed-point problem that can be solved iteratively starting from a reasonable guess for $n(\mathbf{k})$ (e.g., the noninteracting distribution). The Lagrange multiplier μ is determined through an iterative procedure by requiring that the momentum-distribution function integrates to the correct number of electrons. The condition $0 \leqslant n_i \leqslant 1$ is enforced at each step. The integral in Eq. (30) and the evaluation of Eqs. (26) and (27) are performed numerically using the *Mathematica* package [38].

V. RESULTS AND DISCUSSION

In this section we will assess the quality of the PF and W-PF by analyzing the total energies, natural occupation numbers, and band gaps/bandwidths from the EKT using the Hubbard model and the HEG.

A. Hubbard model

In Fig. 1 we report the total energy of a 12-site Hubbard chain, obtained from the direct minimization of the total energy functional given in Eq. (21), as a function of U/t. We notice that only the PF with $\alpha = 0.5$ gives the correct limit for the large-interaction limit $U/t \rightarrow \infty$ [40], while for larger values of α the result diverges. The value $\alpha = 0.5$ also gives the best "global" result. The total energy is hence quite sensitive to the value of α. This is a general trend that is independent of the number of sites.
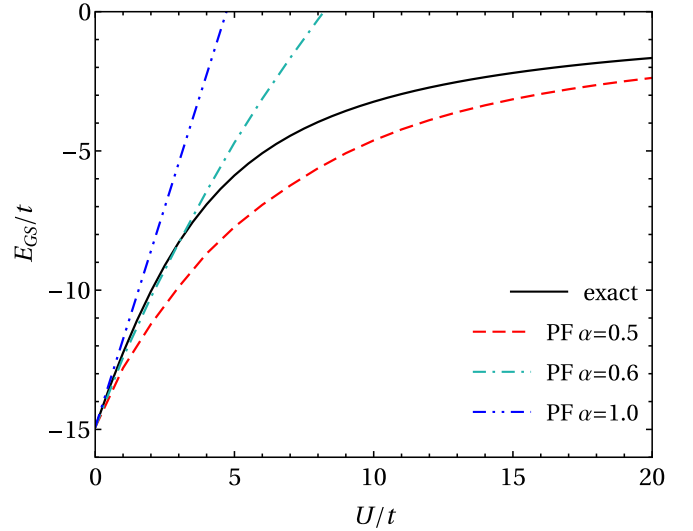

FIG. 1. Total energy as a function of U/t for a 12-site Hubbard chain. Exact vs PF ($\alpha = 0.5$, 0.6, and 1).

The occupation numbers which minimize the total energy functional are reported in Fig. 2 for a 12-site Hubbard chain at $U/t = 4$. Their trends closely resemble those of the infinite chain, also reported in Fig. 2. The PF gives for some states pinned occupation numbers, i.e., $n_i = 1$. In general there is not
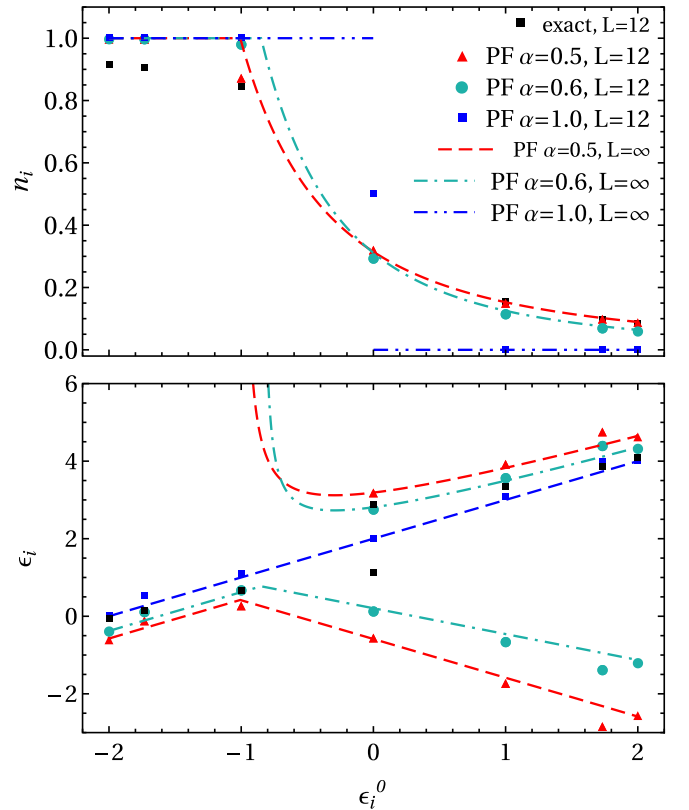

FIG. 2. Occupation numbers (top panel) and removal/addition energies ϵ_i (bottom panel) for a 12-site Hubbard chain and the infinite Hubbard chain at $U/t = 4$. Exact results are reported with black squares for the 12-site Hubbard chain.
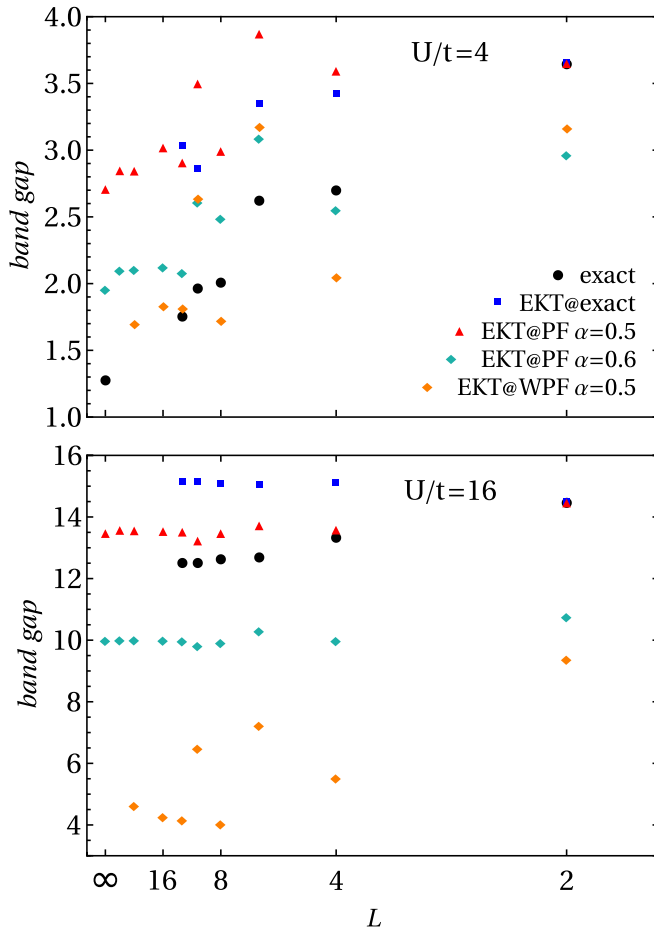
FIG. 3. Fundamental band gap of the one-dimensional Hubbard chain as a function of the length L for $U/t = 4$ and 16: exact results, EKT@exact, and EKT@PF for both $\alpha = 0.5$ and 0.6.

FIG. 4. Correlation energy of the HEG as a function of r_s calculated with the PF and W-PF. The Coulomb hole correction to the W-PF is also reported (W-PF+COH). The quantum Monte Carlo result (QMC) corresponds to the Perdew-Wang fit [41] of the DMC data of Ortiz and Ballone [42,43]. The blue dash-dotted line, for $r_s < 5.77$, is obtained numerically and corresponds to the results by Csányi and Arias [32] employing the Müller functional. The continuation for $r_s > 5.77$ is the analytical result of Cioslowski and Pernal [34].

a large difference between the results obtained with $\alpha = 0.5$ and $\alpha = 0.6$, except for the occupation of the top valence orbital (at $\epsilon_i = -1$). However, we notice a significant difference in the EKT band gap. This is shown in Fig. 3, where we present the band gap of the one-dimensional Hubbard model as a function of the number of sites L for $U/t = 4$ and $U/t = 16$. Exact results are compared with those obtained from the EKT using exact RDMs (EKT@exact) and RDMs obtained from the PF approximation (EKT@PF). For the Hubbard dimer, exact, EKT@exact, and EKT@PF($\alpha = 0.5$) give the same band gap. For more than two sites ($L > 2$) EKT@PF($\alpha = 0.5$) shows the same trend as EKT@exact, i.e., a systematic overestimation of the exact band gap, whose magnitude depends on the strength of the electron correlation. PF($\alpha = 0.6$), instead, gives results closer to the exact ones for $U/t = 4$, whereas it underestimates the band gaps for $U/t = 16$. Overall, these results point to an error cancellation between the approximate nature of the EKT equations and the approximation to the 1- and 2-RDMs by tuning the parameter α. Introducing screening will decrease the gap, as shown in Fig. 3. For example, for the Hubbard dimer screening in PF($\alpha = 0.5$) has an effect similar to using $\alpha = 0.6$ in the PF. In general we observe that the gap shrink induced by the screening increases with the electron correlation.
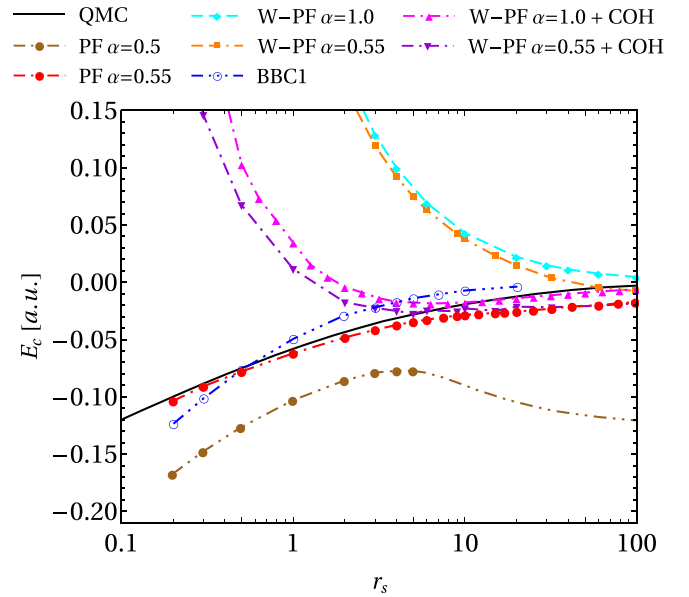
The BBC1 functional produces results (not reported in Fig. 3) in between the results obtained with PF($\alpha = 0.5$) and PF($\alpha = 0.6$). Of course, one should be careful to extrapolate these findings to real materials. This model, indeed, is peculiar because the power functional, which contracts the four-point two-body density matrix to only two points, i.e., $\Gamma^{(2)}_{\text{xc},ijkl} = -n_i^\alpha n_j^\alpha \delta_{ik}\delta_{jl}$, is a good approximation due to the topology of the system; moreover, the basis of natural orbitals is also the basis which diagonalizes the $\mathbf{\Lambda}^{R/A}$ matrices. These features are not generally true in a real system. However, the fact that the EKT method overestimates the exact band gap seems a general feature, as pointed out in Ref. [10], and an important finding. Of course, this also questions its applicability to metals, where there is no band gap. We shall investigate this point with the example of the HEG in the next section.

B. Homogeneous electron gas

We first examine the correlation energy reported in Fig. 4. Our reference is the Monte Carlo (QMC) correlation energy from Ref. [41]. We compare the results obtained using the PF and W-PF. Reference [44] showed that the correlation energy of the HEG is well reproduced by the PF with values of α between 0.55 and 0.58 depending on the value of the Wigner-Seitz radius r_s. We find, indeed, that PF($\alpha = 0.55$) performs very well over a wide range of r_s, unlike PF($\alpha = 0.5$).

For $\alpha = 1$ the W-PF corresponds to the SEX, and it gives positive correlation energies for all densities. Considering $\alpha < 1$ decreases the correlation energy. Moreover, we
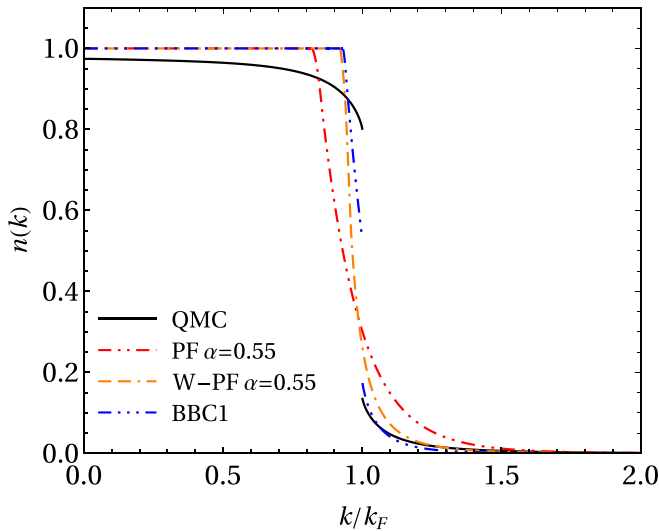
FIG. 5. Momentum distribution of the HEG for $r_s = 3$: QMC vs PF and W-PF for $\alpha = 0.5$ and BBC1. The QMC momentum distribution is taken from Ref. [45].

note that for $\alpha = 0.55$ this functional inherits the correct low-density limit ($r_s \to \infty$) of PF($\alpha = 0.55$) but the incorrect high-density limit ($r_s \to 0$) of the SEX. A similar scenario is observed using the Coulomb hole correction in the W-PF (see Appendix A). Also the correlation energy obtained using BBC1, reported in Fig. 4 as well, compares well with the QMC results over a wide range of r_s values. In Fig. 5 we report the momentum distribution $n(\mathbf{k})$ for $r_s = 3$, for which QMC results (our reference) are available in the literature [45]. We compare the results for QMC and PF and W-PF (both with $\alpha = 0.5$). The PF is not able to describe the characteristic discontinuity of the exact momentum distribution at the Fermi momentum k_F. This is a general feature of the Müller-like functionals. Reference [34], for example, showed that for values of $r_s < 5.77$ the Müller functional produces occupation numbers pinned to 1 for values of k smaller than a characteristic value k_p. For $k > k_p$ the occupation decreases monotonically to zero without discontinuity. As pointed out in Ref. [31], only the BBC functionals have been reported to reproduce this feature. This is, indeed, what we find by using BBC1, which is also reported in Fig. 5. The W-PF improves the situation in the sense that it enlarges the range $0 < k < k_p$, but it cannot reproduce the discontinuity either.

In Fig. 6 we report the quasiparticle (QP) dispersion curve obtained with the EKT. The first remarkable feature that we observe is the opening of an unphysical band gap. The EKT@PF QP dispersion is very close to the HF one for $k < k_p$. Due to the fact that the PF is not able to well reproduce the momentum distribution near $k = k_F$ the QP dispersion is strongly deformed near the Fermi momentum ($k_p < k < k_F$). The range of deformation is, instead, smaller for the W-PF. Moreover, introducing screening in the PF functional reduces the overestimation of the band width, which becomes smaller than the EKT@QMC result. This finding points to an overscreening in the W-PF. Indeed introducing a parameter that reduces the screening in the W-PF would bring the results in

line with the EKT@QMC results, as we show in Appendix B. Nevertheless, the W-PF correctly closes the band gap in the HEG; it would hence be interesting to apply the EKT@W-PF to realistic systems and, in particular, to gapped materials. This study is currently in progress.

Interestingly, the EKT band dispersion obtained using the BBC1 functional is rather bad, at least for the valence part, with respect to the QMC results. Although, similar to the W-PF, BBC1 decreases (but does not close completely) the artificial band gap that the exact EKT method opens in the HEG, the BBC1 band dispersion is quite different from the W-PF dispersion. This is the case also for other values of r_s. We compare our results with the QMC quasiparticle energies obtained from Ref. [47]: W-PF shows a dispersion curvature similar to that of QMC, whereas BBC1 is very similar to HF. We note that also increasing α in the PF tends to close the band gap, with $\alpha = 1$ showing no gap (see Fig. 7). However, this is the HF solution, which is not a good approximation of the 1- and 2-RDM.

In Fig. 8 we also compare our results with the method proposed in Ref. [18] (referred to as the DER method). For valence QP energies this method gives the same expression as EKT@W-PF with W replaced by the parameter α of the PF. The results of the DER method, however, are closer to those obtained using EKT@PF than to the ones obtained using EKT@W-PF, showing that screening has a stronger impact than the α parameter. It would be interesting to explore the use of a static value of W to fix the parameter α in an *ab initio* manner, but that is beyond the scope of the present work.

VI. CONCLUSIONS AND PERSPECTIVES

In this work we explored the influence of the approximations to the 1-RDM and 2-RDM on the removal/addition energies calculated using the extended Koopmans' theorem within reduced density matrix functional theory. In particular we have focused on the power functional approximation to the 2-RDM proposed by Sharma and coworkers, which is often employed in solids. Using the one-dimensional Hubbard chain and the HEG as test systems, we explored the sensitivity of the results to the α parameter of this approximation and the impact of introducing screening in the PF (W-PF). In particular we found the following: (i) In the Hubbard chain the parameter $\alpha = 0.5$ is the best choice for any number of sites when looking at the total energy, the natural occupation numbers, and the EKT band gap. (ii) The EKT energies obtained using exact density matrices show a systematic overestimation of the band gap; for the PF, the larger the interaction is the smaller (towards 0.5) α should be to get good agreement with the exact results, which points to an error cancellation. (iii) Introducing screening reduces the gap in the Hubbard model and improves the quasiparticle dispersion and the bandwidth in the HEG. Although the W-PF does not have a rigorous foundation, our results point to some interesting features for the description of quasiparticle energies. We have also explored the performances of the BBC1 functional, which, as already reported in the literature, well reproduces the correlation energy of the HEG over a wide range of r_s and, at the same time, shows a discontinuity in the occupation number
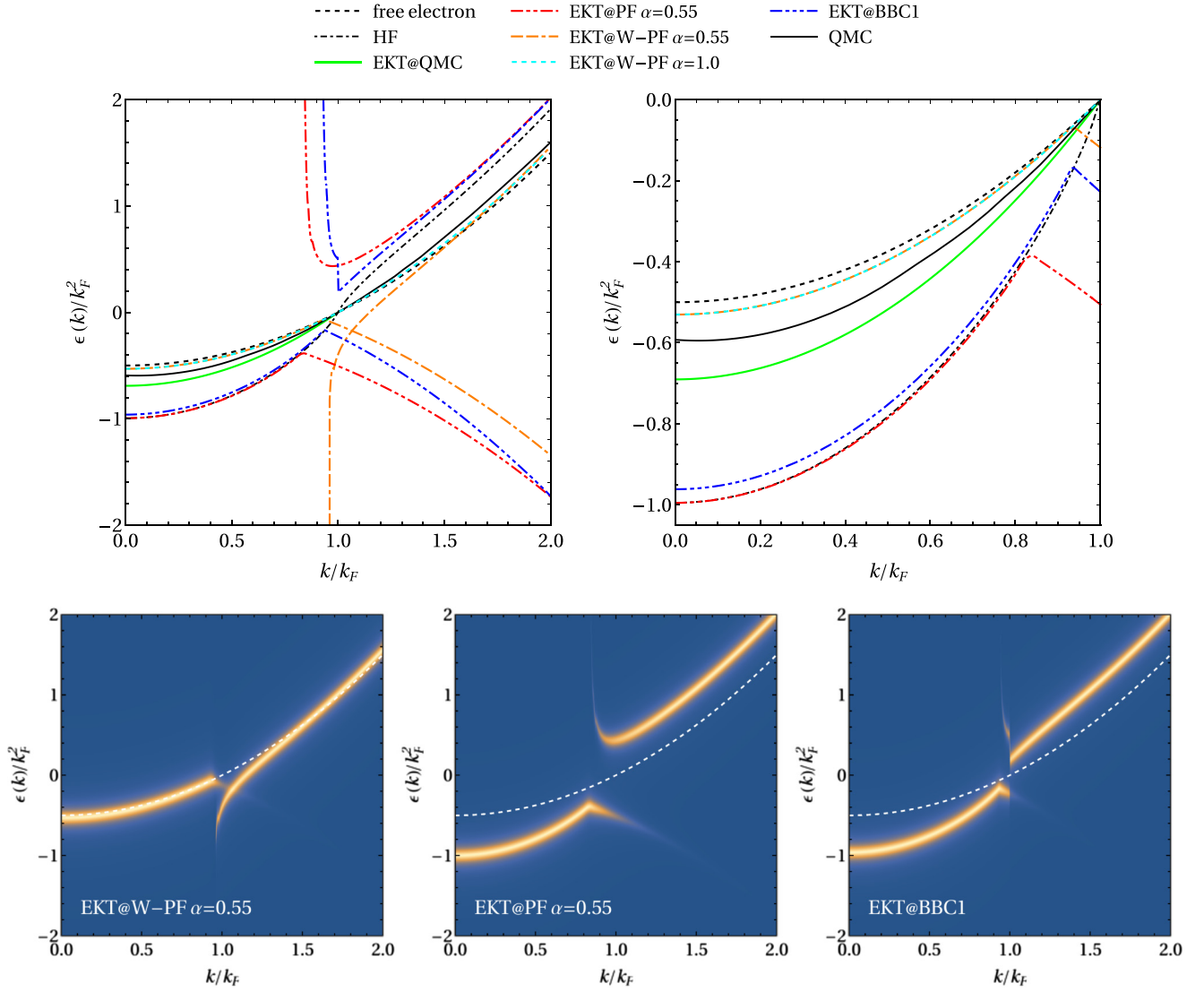
FIG. 6. Quasiparticle dispersion $\epsilon(k)/k_F^2$ for $r_s = 3$: EKT@W-PF, EKT@PF, and EKT@BBC1 are compared with EKT@QMC results extracted from Ref. [46] and QMC quasiparticle dispersion from Ref. [47]. The free-electron and Hartree-Fock dispersions are also reported. In the bottom panels we report the momentum-resolved spectral function $A(\mathbf{k}, \omega)$. The free-electron dispersion is indicated with a dashed white line.

distribution at the Fermi level, as in the exact case. The trend of the EKT removal and addition energies obtained using BBC1 is similar to the one observed using the W-PF for the HEG, in particular the fact that the band gap tends to close compared to the PF. Nevertheless, the band dispersion and bandwidth are quite poor and very similar to those calculated using HF, contrary to the W-PF, which performs quite well. It would be worthwhile to explore the performance of these two functionals in realistic systems. This work is currently in progress.
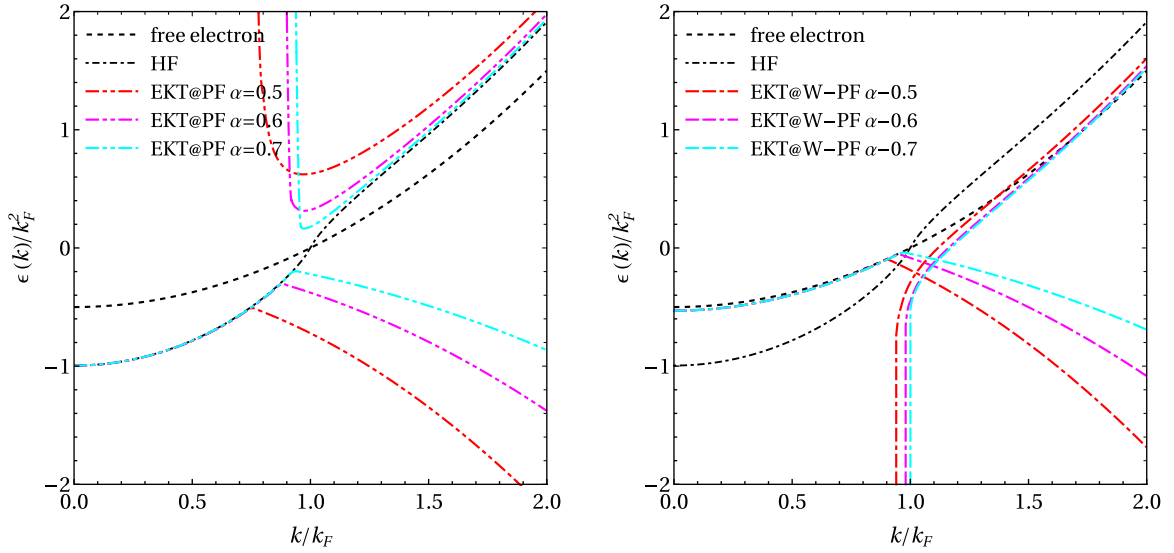
APPENDIX A: THE COULOMB HOLE PLUS SCREENED-EXCHANGE PF

Let us consider the correlation part of W, i.e., $W_p = W - v$. Within the COHSEX approximation to the self-energy the correlation contribution of Eq. (15), in the limit $t_4 = t_1^{+++}$, reads

$$
\sum_i \int dt_2 \Sigma_{c,mi}(t_1 t_2) G_{il}(t_2 - t_4)
$$

$$
= \frac{i}{2} \sum_{ijk} \int dt_2 G_{kj}(t_1 - t_2) W_{p,mjki}(\omega = 0)[\delta(t_1 - t_2 + \eta)
$$

$$
+ \delta(t_1 - t_2 - \eta)] G_{il}(t_2 - t_4)
$$

$$
= \frac{i}{2} \sum_{ijk} [G_{kj}(-\eta) W_{p,mjki} G_{il}(t_1 + \eta - t_4)
$$

$$
+ G_{kj}(\eta) W_{p,mjki} G_{il}(t_1 - \eta - t_4)]
$$

FIG. 7. Dependence of the EKT@PF and EKT@W-PF QP energy dispersions on the parameter α.

$$= \frac{i}{2} \sum_{ijk} [G_{kj}(-\eta)W_{p,mjki}G_{il}(-\eta)$$

$$+ G_{kj}(\eta)W_{p,mjki}G_{il}(-\eta)]$$

$$= \frac{i}{2} \sum_{ijk} [G_{kj}(-\eta)W_{p,mjki}G_{il}(-\eta)$$

$$+ G_{kj}(-\eta)W_{p,mjki}G_{il}(-\eta) - i\delta_{kj}W_{p,mjki}G_{il}(-\eta)]$$

$$= \frac{i}{2} \sum_{ijk} [-2W_{p,mjki}\gamma_{kj}\gamma_{il} + \delta_{kj}W_{p,mjki}\gamma_{il}]. \quad \text{(A1)}$$

By adding the exchange contribution to $\Gamma^{(2)}$ and using the basis of natural orbitals, we arrive at

$$-\sum_j W_{mjjl}n_j n_l + \frac{1}{2}\sum_j W_{p,mjjl}[n_j + n_l]$$

$$= \sum_{ijk} V_{mkij}\Gamma^{(2)}_{c,ijkl}, \quad \text{(A2)}$$

where the first term on the right-hand side is the screened exchange and the second term is the Coulomb hole. As for the SEX-like approximation, in order to get fractional occupation numbers we combine this COHSEX-like approximation with
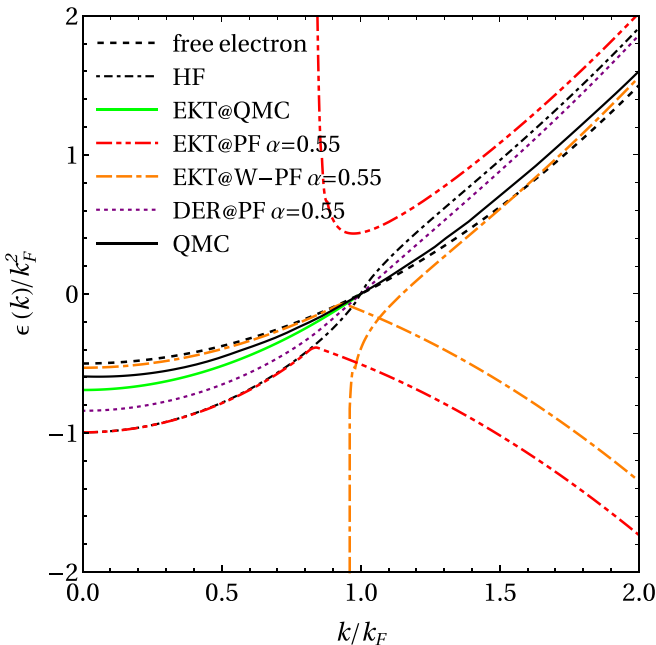
FIG. 8. Quasiparticle dispersion $\epsilon(k)/k_F^2$ for $r_s = 3$: EKT@W-PF and EKT@PF are compared with the DER@PF.
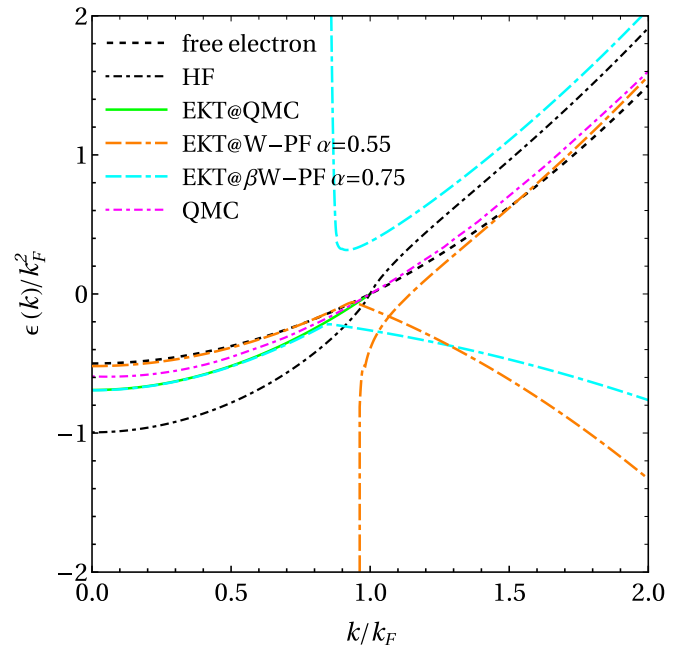
FIG. 9. Quasiparticle dispersion $\epsilon(k)/k_F^2$ for $r_s = 3$: βW-PF is compared with the W-PF.

the PF. One can add the α exponent only to screened-exchange term or, to be more consistent, to the Coulomb-hole term. Here we will consider the α parameter only in the SEX part.

The COHSEX-like approximation is tested in the HEG. In this case the energy functional to be minimized reads

$$
\frac{\mathcal{F}}{\Omega} = \int \frac{d\mathbf{k}}{(2\pi)^3}(\mathbf{k}^2 - 2\mu)n(\mathbf{k})
$$
$$
- \int \frac{d\mathbf{k}d\mathbf{k}'}{(2\pi)^6} v(\mathbf{k} - \mathbf{k}') f(n(\mathbf{k}), n(\mathbf{k}'))
$$
$$
+ \frac{1}{2} \int \frac{d\mathbf{k}'d\mathbf{k}}{(2\pi)^6} W_p(\mathbf{k}')n(\mathbf{k}) + \mu. \quad \text{(A3)}
$$

We notice that Eq. (A3) differs from Eq. (28) by only a term which does not depend on $n(\mathbf{k})$ [$\int d\mathbf{k}n(\mathbf{k})$ is a constant]. This implies that the addition of the Coulomb hole term does not affect the optimal momentum distribution $n(\mathbf{k})$.

APPENDIX B: TUNING THE CORRELATION IN THE HOMOGENEOUS ELECTRON GAS

As discussed in Sec. V B the W-PF suffers by an overscreening problem, which arises from double counting

between W and the PF. Reducing the screening and the correlation in the PF, one can, indeed, find quasiparticle dispersion in agreement with the EKT@QMC results. This can be shown by introducing a parameter β in front of W in the function f as

$$
f^{\beta W-\text{PF}}(n(\mathbf{k}), n(\mathbf{k}')) = \beta \frac{\bar{W}(\mathbf{k} - \mathbf{k}')}{v(\mathbf{k} - \mathbf{k}')}[n(\mathbf{k})n(\mathbf{k}')]^{\alpha}. \quad \text{(B1)}
$$

For a fixed value of α, the parameter β is determined in such a way to obtain the QMC correlation energy of the HEG. The optimal value of α is then determined in such a way to have the same second derivative of $\epsilon^R(\mathbf{k})$ at $\mathbf{k} = 0$ obtained by the EKT@QMC. We find that the optimal values of the two parameters are $\alpha = 0.75$ and $\beta = 5.44$, which indicate a strong reduction of the screening. The results are reported in Fig. 9. One could envisage using (B1) with the parameters β and α optimized for the HEG also for realistic systems in the same spirit as the local density approximation employed in density functional theory.

[1] M. M. Morrell, R. G. Parr, and M. Levy, J. Chem. Phys. **62**, 549 (1975).

[2] D. W. Smith and O. W. Day, J. Chem. Phys. **62**, 113 (1975).

[3] P. R. C. Kent, R. Q. Hood, M. D. Towler, R. J. Needs, and G. Rajagopal, Phys. Rev. B **57**, 15293 (1998).

[4] J. Lee, F. D. Malone, M. A. Morales, and D. R. Reichman, J. Chem. Theory Comput. **17**, 3372 (2021).

[5] K. Pernal and J. Cioslowski, Chem. Phys. Lett. **412**, 71 (2005).

[6] P. Leiva and M. Piris, J. Mol. Struct.: THEOCHEM **770**, 45 (2006).

[7] P.-O. Löwdin, Phys. Rev. **97**, 1474 (1955).

[8] T. L. Gilbert, Phys. Rev. B **12**, 2111 (1975).

[9] K. Pernal and K. J. H. Giesbertz, in *Density-Functional Methods for Excited States*, edited by N. Ferré, M. Filatov, and M. Huix-Rotllant, Topics in Current Chemistry Vol. 368 (Springer, Cham, 2015), pp. 125–183.

[10] S. Di Sabatino, J. Koskelo, J. Prodhon, J. A. Berger, M. Caffarel, and P. Romaniello, Front. Chem. **9**, 819 (2021).

[11] S. Di Sabatino, J. A. Berger, L. Reining, and P. Romaniello, Phys. Rev. B **94**, 155141 (2016).

[12] S. Di Sabatino, J. A. Berger, and P. Romaniello, J. Chem. Theory Comput. **15**, 5080 (2019).

[13] S. Di Sabatino, J. Koskelo, J. A. Berger, and P. Romaniello, Phys. Rev. Research **3**, 013172 (2021).

[14] S. Sharma, J. K. Dewhurst, N. N. Lathiotakis, and E. K. U. Gross, Phys. Rev. B **78**, 201103 (2008).

[15] J. Cioslowski, K. Pernal, and M. Buchowiecki, J. Chem. Phys. **119**, 6443 (2003).

[16] O. Gritsenko, K. Pernal, and E. Baerends, J. Chem. Phys. **122**, 204102 (2005).

[17] Since in the basis of natural orbitals the S^R (S^A) matrix is a diagonal matrix with natural occupation numbers $n_i (1 - n_i)$ as elements, the invertibility of this matrix is strictly related to the

nonexistence of so-called pinned states, i.e., states with occupation numbers equal to 1 or 0. This is an important question that has several consequences [48,49]. Here we assume that S^R (S^A) is invertible in a restricted space (of natural orbitals) in which the corresponding KS orbitals are occupied (unoccupied). This is a reasonable assumption.

[18] S. Sharma, J. K. Dewhurst, S. Shallcross, and E. K. U. Gross, Phys. Rev. Lett. **110**, 116403 (2013).

[19] A. Müller, Phys. Lett. A **105**, 446 (1984).

[20] M. Piris, Int. J. Quantum Chem. **106**, 1093 (2006).

[21] M. Piris, Phys. Rev. Lett. **119**, 063002 (2017).

[22] M. Piris, Phys. Rev. Lett. **127**, 233001 (2021).

[23] G. Strinati, Riv. Nuovo Cimento **11**, 1 (1988).

[24] S. Di Sabatino, J. A. Berger, L. Reining, and P. Romaniello, J. Chem. Phys. **143**, 024108 (2015).

[25] L. Hedin, Phys. Rev. **139**, A796 (1965).

[26] M. S. Hybertsen and S. G. Louie, Phys. Rev. B **34**, 5390 (1986).

[27] L. Hedin, J. Phys.: Condens. Matter **11**, R489 (1999).

[28] J. A. Berger, P.-F. Loos, and P. Romaniello, J. Chem. Theory Comput. **17**, 191 (2021).

[29] S. D. Sabatino, Ph.D. thesis, Université Toulouse III-Paul Sabatier, 2015.

[30] Note that this formula is valid only for $L > 2$. For $L = 2$ we have $\epsilon_1 = -t$ and $\epsilon_2 = +t$.

[31] N. N. Lathiotakis, N. Helbig, and E. K. U. Gross, Phys. Rev. B **75**, 195120 (2007).

[32] G. Csányi and T. A. Arias, Phys. Rev. B **61**, 7348 (2000).

[33] G. Csányi, S. Goedecker, and T. A. Arias, Phys. Rev. A **65**, 032510 (2002).

[34] J. Cioslowski and K. Pernal, J. Chem. Phys. **111**, 3396 (1999).

[35] J. Lindhard, K. Dan. Vidensk. Selsk., Mat.-Fys. Medd. **28** (1954).

[36] G. Alvarez, DMRG++, https://g1257.github.io/dmrgPlusPlus/.

[37] E. H. Lieb and F. Y. Wu, Phys. Rev. Lett. **20**, 1445 (1968).

[38] Wolfram Inc., *Mathematica*, Version 12.3.1, Champaign, IL, 2021.

[39] Note that for $\alpha = 1$ Eq. (29) cannot be used to derive the fixed-point equation (30). In this case the solution is given by the HF solution $n(\mathbf{k}) = \theta(k_F - |\mathbf{k}|)$.

[40] For $U/t \to \infty$ the exact energy vanishes; in fact, each electron localizes on one site, and double occupancy is not allowed (we assumed that the site orbital energy is zero). In the approximate functional given in Eq. (21), for $U/t \to \infty$ the kinetic term is negligibly small compared to the exchange-correlation term. Since n_i are symmetric, the optimal occupation numbers are $n_i = N/L = 1/2$. Substituting this value in the energy functional, we obtain $E = 0$.

[41] J. P. Perdew and Y. Wang, Phys. Rev. B **45**, 13244 (1992).

[42] G. Ortiz and P. Ballone, Phys. Rev. B **50**, 1391 (1994).

[43] G. Ortiz and P. Ballone, Phys. Rev. B **56**, 9970(E) (1997).

[44] N. N. Lathiotakis, S. Sharma, J. K. Dewhurst, F. G. Eich, M. A. L. Marques, and E. K. U. Gross, Phys. Rev. A **79**, 040501(R) (2009).

[45] P. Gori-Giorgi and P. Ziesche, Phys. Rev. B **66**, 235116 (2002).

[46] J. T. Krogel, J. Kim, and F. A. Reboredo, Phys. Rev. B **90**, 035125 (2014).

[47] S. Azadi, N. D. Drummond, and W. M. C. Foulkes, Phys. Rev. Lett. **127**, 086401 (2021).

[48] K. J. H. Giesbertz and R. van Leeuwen, J. Chem. Phys. **139**, 104109 (2013).

[49] T. Baldsiefen, A. Cangi, and E. K. U. Gross, Phys. Rev. A **92**, 052514 (2015).